Microwave-assisted synthesis of Bis-histidinato nickel (II) complex and its luminescence properties

Coddy Cash[1], Hashini N. K. Herath[1], Harshica Fernando[1], Gina M. Chiarella[1]*,
Lihong Zhang[2], Liang Yang[3], Hua-Jun S. Fan[3]*

[1] *Department of Chemistry and Physics, Prairie View A&M University, Prairie View, TX, USA*
[2] *Department of gastroenterology, Binhai New Area Hospital of TCM Tianjin, Tianjin, P. R. China, 300451*
[3] *College of Chemical Engineering, Sichuan University of Science and Engineering, Zigong City, Sichuan Province, P. R. China, 64300*

Abstract:
Metal complexes of biological molecules are a topic in demand for environmental purposes. Modern chemistry looks for the eco-friendly preparation of green compounds with optical and electrochemical properties with applications in technological fields. Herein, we prepared a metal complex bis-histidinato nickel (II) (BHN) from nickel(II) acetate and L-histidine using a non-contaminant microwave-assisted technique. By taking advantage of efficient and controlled heating provided by microwave-assisted synthesis, a quality crystal of BHN was obtained and the resolution of the crystal structure of this complex showed an R1 = 0.0155 and wR2 = 0.0410. Crystal Data for $C_{12}H_{18}N_6NiO_5$ (M = 385.03 g/mol): monoclinic, space group C2 (no. 5), a = 29.3180(12) Å, b = 8.2185(3) Å, c = 6.2729(3) Å, β = 90.0630(10)°, V = 1511.45(11) Å³, Z = 4, T = 110.0 K, μ(MoKα) = 1.323 mm⁻¹, ρcalc = 1.692 g/cm³, 23159 reflections measured (6.478 ° ≤ 2Θ ≤ 54.972 °), 3369 unique (R_{int} = 0.0262, R_{sigma} = 0.0203) which were used in all calculations. The final R1 was 0.0155 (I > 2σ(I)) and wR2 was 0.0410 (all data). The luminescence spectra of BNH suggested that π–π stacking interactions between imidazole rings of neighboring molecules favored by the presence of hydrogen bonds.
Key words: Nickel-L-histidine complex, microwave assisted synthesis, x-ray single crystal determination, Luminescence

I. Introduction

Since its inception, microwave-assisted chemical synthesis has become well-established practices in the laboratory setting [1,2]. Hailed as the Bunsen burner of the 21st century, the microwave-assisted synthesis technique has emerged as a valuable alternative in the synthesis of organic compounds [3], polymers [4], inorganic materials [5], and nanomaterials [6,7,8]. Instead of using conventional heating methods such as gas Bunsen burners, ovens, water or oil bath, and hotplate, microwave using microwave radiation to provide alternative heating and energy for reaction to occur. Because microwaves are a form of electromagnetic radiation with a frequency between radio waves and infrared radiation, microwave-assisted synthesis relies on the selective absorption of microwave energy by molecules with dipolar or polar properties. As such, it can heat the reaction mixture very quickly and uniformly, which result in faster reaction rates, improved reaction yield, reduction of side reaction, and selective activation of specific reactants. It can be used in the solvent-free and water-mediated reactions [9,10,11,12,13]. Therefore, microwave-assist synthesis will reduce the chemical waste, increase energy efficiency, and have a more positive impact on the environment compared to some traditional synthesis methods. Recently, applying microwave-assisted synthesis on nanomaterials and catalysts have gained momentum because of growth of these materials requires specific reaction conditions by taking advantage of efficient and controlled heating provided by microwave-assisted synthesis [14].

Nanomaterials, metal nanoparticles, and nanostructures have a wide range of applications across various fields such as electronics, photonics in solar cells and catalysts in materials science due to their unique properties and versatility. Particularly, the quest for new eco-friendly catalysts [15], the pursuit of green new materials with optical properties [16], and the search for environmentally safe compounds with possible applications in pharmacological [17] and nutritional fields are goals of environmental remediation and sustainability alternatives [18] to save our planet from ecological disasters. This makes the microwave-assisted synthesis quite an attractive synthesis technique to be deployed in this arena.

On the other hand, metal ions coordinated with amino acids can catalyze a wide range of biochemical reactions like energy production, DNA replication [19], and molecular transport [20] in biological systems. The metal center of the metalloenzyme provides the needed structural environment to catalyze reactions by forming metal-binding sites. Researchers use to mimic the core structures of them to study their possible applications. It is one of research area intensively pursued by the researchers around the word. For example, Nickel amino acid compounds play crucial roles in biological systems due to their significance in various biochemical processes; especially in enzymes known as nickel-dependent enzymes. They can serve as cofactors, as in acetyl CoA synthetase [21] and in the quercetin 2,4-dioxygenase where a nickel(II) ion coordinated to three imidazole nitrogen from histidine groups and a glutamate residue and catalyzes oxidative cleavage of quercetin [22]. In Hydrolases as urease [23,24,25]. In electron transfer enzymes such as nickel-hydrogenase, methyl-coenzyme M reductase [10]. They are also present in oxidoreductases such as superoxide dismutase [26], acireductone dioxygenase [27], CO dehydrogenase [28]; in isomerases as glyoxalase I [29] and lactate racemase [30].

As an essential amino acid [31], L-histidine plays an important part in the biosynthesis of proteins. The deficiency of this amino acid is fatal in children and leads to chronic renal failure in adults [32]. L-Histidine is present in almost 50% of active sites of enzymes [33], and the side-chain, imidazole ring, plays a crucial role in the stability and functionality of the amino acid in the proteins. It is well known that the N-donor atoms of the imidazole group are the exclusive binding sites for metals below pH 7.5. Above that value, the nitrogen atom of the amino group of this amino acid also binds transition metals [34]. Different reaction conditions and ligand would result in different binding environment at the metal center. Therefore, this metal-containing amino acid complex is an ideal candidate for the microwave-assisted technique.

In this study, we will employ microwave-assisted technique to synthesize the Bis-L-histidinato nickel (II) (BHN) at different pH values. Because the different pH and reaction condition will influence the outcome and quality of products, the synthesis procedure will be modified from the traditional refluxing method by taking advantage of by taking advantage of efficient and controlled heating provided by microwave-assisted synthesis. The reaction investigated in this study is shown in Figure 1. The luminescence spectrum will be used to measure the optical property of the BHN.
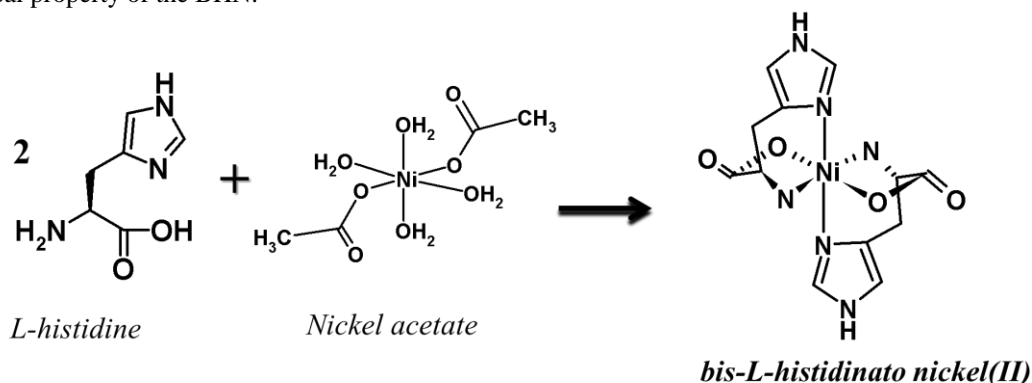
Figure 1 Stoichiometric reaction for the preparation of BHN

II. Experimental section

2.1. Materials and methods

All chemicals utilized in this work were analytical grade reagents and purchased from commercial sources; L-histidine was purchased from J.T. Baker; Nickel (II) Acetate Tetrahydrate from Acros Organics, potassium hydroxide from E.M. Science. Buffers phosphate (pH 7.4) and carbonate-bicarbonate (pH 10) were prepared in our laboratory.

All operations were carried out in ambient conditions. Synthetic procedures were executed using a classical refluxing apparatus and microwave synthesizer. The crystal structure recording and determination were executed at the Department of Chemistry at Texas A&M University. The UV-vis spectroscopy was measured in a Jasco V-770 spectrophotometer.

2.2. Synthetic procedures

The BHN was prepared by the reaction of 0.00135 moles of Nickle acetate tetrahydrate (0.34 g) with a solution of 0.0027 moles of L-histidine (0.42 g dissolved in 20 mL water), the procedure took place using two different methods, a) in a microwave synthesizer and b) by reflux in water.

2.2.1. Crystal Structure determination and refinement

Single crystals of $C_{12}H_{18}N_6NiO_5$ [BHN] were grown in water solution by deposition. After two days a purple needle plate shaped crystal of 0.4, 0.165, 0.13 mm suitable was selected and mounted on a Bruker Photon 3 area detector diffractometer. The crystal was kept at 110.0 K during data collection. Using Olex2 [35], the structure was solved with the XT [36] structure solution program using Intrinsic Phasing and refined with the XL [37] refinement package using Least Squares minimization. This compound crystallized in the monoclinic space group C2 (C121).

Crystallographic data for BHN has been deposited with the Cambridge Crystallographic Data Centre, CCDC reference number 2288361, DOI: 10.5517/ccdc.csd.cc2gt73n. Copies of the data can be obtained free of charge on application to CCDC, 12 Union Road, Cambridge CB2 1EZ, UK (fax: (44) 1223 336-033; e-mail: deposit@ccdc.cam.ac.uk).

2.2.2. Luminescence measurements

The luminescence spectra of BHN at pH 7 and 10, and L-histidine, were recorded using a Jasco FP- 8300(ST) spectrofluorometer with Spectra Manager II in water solution with the following specifications, for L-histidine the measurement range was from 250 to 600 nm, with the excitation wavelength at 230 nm; in both BHN experiments the measurements were perform in the range of 300 to 600 nm, with the excitation wavelength at 350 nm; in all experiments the scan speed was 1000 nm/min

III.   Results and discussion

3.1. Preparation and crystallization

The preparation of BHN is carried out by adding nickel acetate to a solution of L-histidine in a sealed tube and microwaving it at 1 atmosphere and 40°C for 20 minutes; when the reaction finished, the reacting mixture changed into a faded purple color soluble in water. Drops of 1 M potassium hydroxide solution are added to 20 mL of the reaction mixture (until it reaches pH 10). A similar result occurs by refluxing the same reactants in water for two to three days. Once the reaction ended, the solid was filtered to remove the excess unreacted amino acid and metal salt, washed with 5 mL of cold water three times and dried at room temperature. In both cases the resulting mixtures contained pink-purple solids.

Comparison of the microwave-assisted technique with the traditional refluxing procedure underlined the advantage of a microwave synthesis not only for the speed of the reaction (20 minutes against the 70 hours in the last one) but also because the microwave-assisted technique is energy-saving and environmental safety, which avoids possible spills and vapor gases usually produced during the refluxing procedure.

In both procedures, the pH was raised to 10 by adding a 1.0 molar concentration of potassium hydroxide to accelerate the formation of crystals. The yield of the preparation using a microwave synthesizer was 90%. The recorded crystal structure is shown in Fig 2. Although the crystal structure of BHN is already published, the published crystal data was with a lower sensitivity. However, better quality crystal structure is needed in order to seek the spectroscopic and electrochemical properties of BHN. Single purple crystals grew by settling down a concentrated aqueous solution from the filtrate in a vial for almost two days at pH 10. An alternative method was the crystallization by vapor diffusion of a water-solution of the compound with methanol. Crystal Data for $C_{12}H_{18}N_6NiO_5$ (M = 385.03 g/mol): monoclinic, space group C2 (no. 5), a = 29.3180(12) Å, b = 8.2185(3) Å, c = 6.2729(3) Å, β = 90.0630(10)°, V = 1511.45(11) Å^3, Z = 4, T = 110.0 K, μ(MoKα) = 1.323 mm^{-1}, ρcalc = 1.692 g/cm^3, 23159 reflections measured (6.478 ° ≤ 2Θ ≤ 54.972 °), 3369 unique (R_{int} = 0.0262, R_{sigma} = 0.0203) which were used in all calculations. The final R1 was 0.0155 (I > 2σ(I)) and wR2 was 0.0410 (all data)
The asymmetric unit consists of one molecule of BHN hydrogen bonding to a molecule of water. Crystal structure refinement and final information are presented in Table 1.
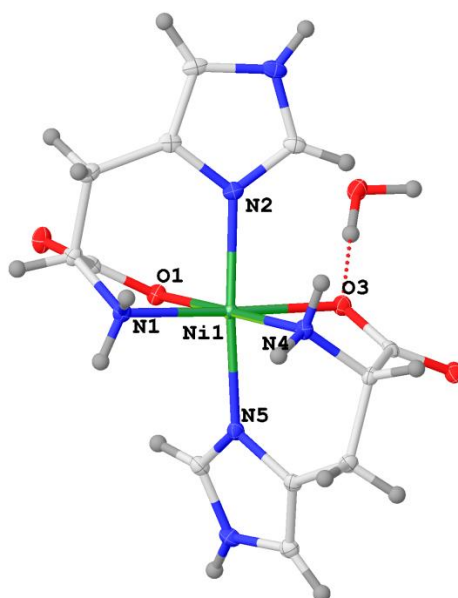
Figure 2 Crystal structure of BHN showing thermal ellipsoids at 50% (OLEX2)

| Table 1: Crystal structure information of BHN	
Empirical Formula	$C_{12}H_{18}N_6NiO_5$
Molar mass	385.03 g/mol
Crystal system	monoclinic
Space group	C2
Z	4
a/Å	29.3180(12)
b/ Å	8.2185(3)
c/ Å	6.2729(3)
β	90.0630(10)°
Cell volume	1511.45(11) Å^3
Final R index (all data)	R1 = 0.0155, wR2 = 0.0410
Goodness-of-fit on F^2	1.050

3.2 Structures at Nickel center

From the crystal structure shown in Figure 2, one can see that the nickel center displays an octahedral-distorted geometry that binds one oxygen atom from the carboxylic group, the nitrogen 1 (and 4 from the other histidine) from the amino group, and the nitrogen delta (2) (and 5 from the other histidine) from the imidazole rings. Due to the presence of water molecules in the structure and the highly electronegative atoms such as oxygen and nitrogen, the crystal structure shows several hydrogen bonds and short contacts. Each water molecule in the structure forms three hydrogen bonds with BHN units, two of them through the hydrogen atoms of the water with a carboxylic oxygen atom attached to the nickel (II) center and with the free oxygen atom of another BHN unit; the third hydrogen bond is between the oxygen atom from the water and the hydrogen attached to the nitrogen-epsilon atom (N3 in one histidine an N6 in the other one), of the imidazole group. There are other hydrogen bonds between carboxylic and amino groups of adjacent molecules.

In the b axes of the crystallographic cell, the angle between imidazole rings of two adjacent molecules is 75.74°, and the distance between those rings is 4.830 Å. The distance between imidazole rings in two parallel molecules is 6.488Å. In the c axes, the angle between two imidazole rings in two adjacent molecules is closely 0°; these rings are located in a parallel displacement array and at the distance of 3.451Å, which is considered a stable configuration for a π-π staking interaction [38,39]. The perfectly closest distance between parallel imidazole rings is at 6.260Å in a sandwich array; in this case, the distance between rings and the arrangement does not fit the requirement for π-π staking interaction.

3.3 Luminescence

Comparing the spectra of the BHN complex with the free L-histidine, the luminescence emissions appear at different wavelengths. As shown in Figure 3, the luminescence of L-histidine (Fig. **3A**) in water at 312 nm (with excitation wavelength at 230 nm), while the BHN complex emits at 422 nm at pH 7 (Fig. **3B**) and 425 nm at pH 10 (Fig. **3C**). The compound did not present luminescence at 550 nm at any pH measured. In his work about luminescence of L-histidine, Iwunze [40] reported the fluorescence emission of L-histidine at 360 nm; he experimented with simulated body fluid at an excitation wavelength of 220 nm. Though the peak was not highly intense, it was strong enough to study the interaction of L-histidine with hydrogen peroxide. Iwunze's report is close to the measurements of the L-histidine in this work; the difference is that this work use water as the solvent and the excitation wavelength of 230 nm. Other the other hand, Wegeberg and Wenger [41] indicated that nickel(II) is among the first-row transition metals able to display luminescence, especially in square planar compounds, the luminescence in these cases is strong at low temperatures, but at room temperature luminescence emissions are rare. Luminescence behavior in Nickel(II) occurs in macrocyclic compounds [42], supramolecular assembly units containing this ion [43], in layered organic-inorganic oligophenylenevinylene nickel(II) compounds [44].
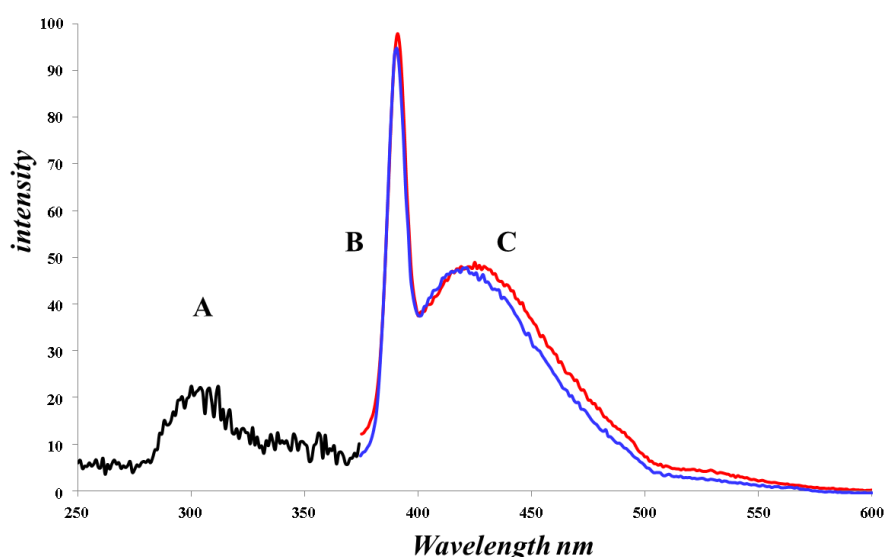
Figure 3 Luminescence spectra in water solution, A) in black luminescence spectrum of L-histidine, B) in blue luminescence spectrum of BHN at pH 7, C) in red, luminescence spectrum of BHN at pH 10

As in most luminescent materials, this optical property arises from aromatic groups and π-delocalized electronic systems present in the structure, which are listed as fluorophore moieties of fluorescent species. Biomolecules with luminescent properties are of great interest in biological markers manufacturing, molecular recognition uses, separation of biomolecules, and biological and non-biological sensors preparation [45,46]. Due to this property, L-histidine is also used to prepare bio-conjugated quantum dots and reagents for immunoassays [47] when combined with metal-sulfur or selenium core-shell quantum dots. The source of the L-histidine luminescence property is the presence of the imidazole ring in the side chain of this amino acid [48, 49]. Experiments executed on free L-histidine reported a weak intensity of the emission spectrum [**Error! Bookmark not defined.**] enhanced by the addition of strong fluorophore inductors as o-Phthalaldehyde (OPT) [50] or 4'-phenylspiro[2-benzofuran-3,2'-furan]-1,3'-dione (fluorescamine) [56] and more recently by the addition of doped metalorganic frameworks as luminescence turn-on sensor for L-histidine detection [48, 51, 52], or by acid hydrolysis [53].

In this work, the crystal structure of BHN shows π–π stacking interactions between imidazole rings of neighboring molecules favored by the presence of hydrogen bonds. Several histidine derivatives exhibit enhanced luminescence, as is reported in cases of histidine-containing peptides [54, 55]. However, most of these compounds undergo a decrease in the intensity of the emitted light or completely quenched luminescence due to the presence of paramagnetic species. Those cases comprise a variety of situations going from the binding of paramagnetic metal ions to the amino acid to the presence of oxygen molecules in the testing solution, a property used in the preparation of probes for L- Histidine detection [56]. Most of these probes contain paramagnetic ions in their structures.

According to the Yang et. al. theory on fluorescence regulation mechanism for paramagnetic ions [57], the source for quenching of fluorescence emission is the competition of non-radiative decay transitions when the mixed fluorophore-metal $^3\pi\pi^*/dd$ state has a similar energy to the fluorophore-localized $^1\pi\pi^*$ state. However, if the exited energy level of the paramagnetic metal has lower energy than the excited state energy of the fluorophore, the quenching would not occur. For example, in a paper on luminescence of L-histidine, Loewenthal and coworkers 54 found changes in the luminescence spectra of L-histidine derivatives by the effect of the pH of the tested sample; this work explored the possibility of pH effect in the luminescence emission of this metal complex, which showed a slight shift from 422 to 425 nm when the pH increases from 7 to 10.

IV. Conclusion

The pursuit of ecologically friendly catalysts and luminescent compounds is an urgent need to face the nowadays environmental challenge. This study employed microwave-assisted synthesis technique to synthesize and crystalize a quality bis-L-histidine Nickel(II) (BHN) complex, a far better quality data than previous published data. Crystal Data for $C_{12}H_{18}N_6NiO_5$ (M = 385.03 g/mol): monoclinic, space group C2 (no. 5), a = 29.3180(12) Å, b = 8.2185(3) Å, c = 6.2729(3) Å, β = 90.0630(10)°, V = 1511.45(11) Å^3, Z = 4, T = 110.0 K, μ(MoKα) = 1.323 mm^{-1}, ρcalc = 1.692 g/cm^3, 23159 reflections measured (6.478 ° ≤ 2Θ ≤ 54.972 °), 3369 unique (R_{int} = 0.0262, R_{sigma} = 0.0203) which were used in all calculations. The final R1 was 0.0155 (I > 2σ(I)) and wR2 was 0.0410 (all data). The luminescence spectra of BNH suggested that π–π stacking interactions between imidazole rings of neighboring molecules favored by the presence of hydrogen bonds.

References

[1]. Gedye, R.; Smith, F.; Westaway, K.; Ali, H.; Baldisera, L.; Laberge, L.; Rousell, J. The use of microwave-ovens for rapid organic-synthesis. Tetrahedron Lett. 1986, 27, 279– 282. https://doi.org/10.1016/S0040-4039(00)83996-9.

[2]. Giguere, R. J.; Bray, T. L.; Duncan, S. M.; Majetich, G. Application of commercial microwave-ovens to organic-synthesis Tetrahedron Lett. 1986, 27, 4945– 4948. https://doi.org/10.1016/S0040-4039(00)85103-5

[3]. Polshettiwar, V.; Nadagouda, M. N.; Varma, R. S. Microwave-assisted chemistry: A rapid and sustainable route to synthesis of organics and nanomaterials Aus. J. Chem. 2009, 62, 16– 26. https://doi.org/10.1071/CH08404

[4]. Virkutyte, J.; Varma, R. S. Green synthesis of metal nanoparticles: Biodegradable polymers and enzymes in stabilization and surface functionalization Chem. Sci. 2011, 2, 837– 846. https://DOI: 10.1039/C0SC00338G

[5]. Nadagouda, M. N.; Speth, T. F.; Varma, R. S. Microwave-assisted green synthesis of silver nanostructures Acc. Chem. Res. 2011, 44, 469– 478. https://doi.org/10.1021/ar1001457

[6]. Baruwati, B.; Varma, R. S. High value products from waste: Grape pomace extract-a three-in-one package for the synthesis of metal nanoparticles ChemSusChem 2009, 2, 1041– 1044. https://doi.org/10.1002/cssc.200900220

[7]. Baruwati, B.; Polshettiwar, V.; Varma, R. S. Glutathione promoted expeditious green synthesis of silver nanoparticles in water using microwaves Green Chem. 2009, 11, 926– 930. https://doi.org/10.1039/B902184A

[8]. Kou, J. H.; Varma, R. S. Beet juice-induced green fabrication of plasmonic AgCl/Ag nanoparticles ChemSusChem 2012, 5, 2435– 2441. https://doi.org/10.1002/cssc.201200477

[9]. Gawande, M. B.; Bonifacio, V. D. B.; Luque, R.; Branco, P. S.; Varma, R. S. Benign by design: Catalyst-free in-water, on-water green chemical methodologies in organic synthesis Chem. Soc. Rev. 2012, 42, 5522– 5551. https://doi.org/10.1039/C3CS60025D

[10]. Gawande, M. B.; Bonifacio, V. D. B.; Luque, R.; Branco, P. S.; Varma, R. S. Solvent-free and catalysts-free chemistry: A benign pathway to sustainability ChemSusChem 2014, 7, 24– 44. https://doi.org/10.1002/cssc.201300485

[11]. Polshettiwar, V.; Varma, R. S. Aqueous microwave chemistry: A clean and green synthetic tool for rapid drug discovery Chem. Soc. Rev. 2008, 37, 1546– 1557. https://doi.org/10.1039/B716534J

[12]. Gawande, M. B.; Branco, P. S. An efficient and expeditious Fmoc protection of amines and amino acids in aqueous media Green Chem. 2011, 13, 3355– 3359. https://doi.org/10.1039/C1GC15868F

[13]. Polshettiwar, V.; Varma, R. S. Tandem bis-aldol reaction of ketones: A facile one-pot synthesis of 1,3-dioxanes in aqueous medium J. Org. Chem. 2007, 72, 7420– 7422. https://doi.org/10.1021/jo701337j

[14]. Manoj B. Gawande, Sharad N. Shelke, Radek Zboril, and Rajender S. Varma, Microwave-Assisted Chemistry: Synthetic Applications for Rapid Assembly of Nanomaterials and Organics, Acc. Chem. Res. 2014, 47(4), 1338–1348. https://doi.org/10.1021/ar400309b

[15]. Hu, Y.; Hu, P.; Zhang, Y.; Xue, N. Short flow and eco-friendly process for V2O3 preparation via hydrogen-catalyzed solution-phase method. **2023**, 307, 122676-122688. https://doi.org/10.1016/j.seppur.2022.122676

[16]. Barzinjy, A. A.; Hamad, S. M.; Aydin, S.; Ahmed, M. H.; Hussain, F. H. S. Green and eco-friendly synthesis of Nickel oxide nanoparticles and its photocatalytic activity for methyl orange degradation. J Mater Sci-Mater El. **2020**, 31, 14, 11303-11316. https://doi.org/10.1007/s10854-020-03679-y

[17]. El Shafey, A. M. Green synthesis of metal and metal oxide nanoparticles from plant leaf extracts and their applications: A review. Green Process Synth. **2020**, 9, 304–339. https://doi.org/10.1515/gps-2020-0031

[18]. Pandey, A. K.; Gaur, V. K.; Udayan, A.; Varjani, S.; Kim, S.-H.; Wong, J. W. C. Biocatalytic remediation of industrial pollutants for environmental sustainability: Research needs and opportunities. Chemosphere. **2021**, 272, 129936-129948. https://doi.org/10.1016/j.chemosphere.2021.129936

[19]. Valdez, C. E.; Smith, Q. A.; Nechay, M. R.; Alexandrova, A. N. Mysteries of Metals in Metalloenzymes. Acc. Chem. Res. **2014**, 47, 10, 3110-3117. https://doi.org/10.1021/ar500227u

[20]. Reetz, M. T. Directed Evolution of Artificial Metalloenzymes: A Universal Means to Tune the Selectivity of Transition Metal Catalysts?. Acc. Chem. Res. **2019,** 52, 2, 336-344. https://doi.org/10.1021/acs.accounts.8b00582

[21]. Manesis, A. C.; Musselman, B. W.; Keegan, B. C.; Shearer, J.; Lehnert, N.; Shafaat, H. S. A Biochemical Nickel(I) State Supports Nucleophilic Alkyl Addition: A Roadmap for Methyl Reactivity in Acetyl Coenzyme A Synthase. Inorg. Chem. **2019**, 58, 14, 8969-8982. https://doi.org/10.1021/acs.inorgchem.8b03546

[22]. Jeoung, J-H.; Nianios, D.; Fetzner, S.; Dobbek, H. Quercetin 2,4-Dioxygenase Activates Dioxygen in a Side-On O2–Ni Complex. Angew Chem Int Edit. **2016**, 55, 10, 3281-3284. https://doi.org/10.1002/anie.201510741

[23]. Walsh, C. T.; Orme-Johnson, W. H. Nickel enzymes. Biochemistry. **1987**, 26, 16, 4901-4906. https://doi.org/10.1021/bi00390a001

[24]. Siegbahn, P. E. M.; Chen, S-L.; Liao, R-Z. Theoretical Studies of Nickel-Dependent Enzymes. Inorganics. **2019**, 7, 8, 95-124. https://doi.org/10.3390/inorganics7080095

[25]. Ragsdale, S. W. Nickel-based Enzyme Systems. J Biol Chem. **2009**, 284, 28, 18571-18575. https://doi.org/10.1074/jbc.R900020200

[26]. Barondeau, D. P.; Kassmann, C. J.; Bruns, C. K.; Tainer, J. A.; Getzoff, E. D. Nickel Superoxide Dismutase Structure and Mechanism. Biochemistry. **2004**, 43, 25, 8038-8047. https://doi.org/10.1021/bi0496081

[27]. Ivan, D. A.; Gremillion, A. J.; Sanchez, A.; Sanchez, S.; Lynch, V. M.; Toledo, S. A. The first structural model for the resting state of the active site of nickel acireductone dioxygenase (Ni-ARD). Inorg Chem Commun. **2018,** 89, 37-40. https://doi.org/10.1016/j.inoche.2018.01.014

[28]. Can, M.; Armstrong, F. A.; Ragsdale, S. W. Structure, Function, and Mechanism of the Nickel Metalloenzymes, CO Dehydrogenase, and Acetyl-CoA Synthase. Chem. Rev. **2014**, 114, 8, 4149-4174. https://doi.org/10.1021/cr400461p

[29]. Clugston, S. L.; Barnard, J. F. J.; Kinach, R.; Miedema, D.; Ruman, R.; Daub, E.; Honek, J.F. Overproduction and Characterization of a Dimeric Non-Zinc Glyoxalase I from Escherichiacoli: Evidence for Optimal Activation by Nickel Ions. Biochemistry. **1998**, 37,24, 8754-8763. https://doi.org/10.1021/bi972791w

[30]. Desguin, B.; Zhang, T.; Soumillion, P.; Hols, P.; Hu, J.; Hausinger, R. P. A tethered niacin-derived pincer complex with a nickel-carbon bond in lactate racemase. Science. **2015**, 349, 6243, 66-69. https://doi.org/10.1126/science.aab2272

[31]. Young, V. R. Adult amino acid requirements: the case for a major revision in current recommendations. J Nutr. **1994**, 124, 8S, 1517S-1523S. https://doi.org/10.1093/jn/124.suppl_8.1517S

[32]. Kopple, J. D.; Swendseid, M. E. Evidence that histidine is an essential amino acid in normal and chronically uremic man. J Clin Invest. **1975**, 55, 5, 881-91. https://doi.org/10.1172/JCI108016

[33]. Hansen, A. L.; Kay, L. E. Measurement of histidine pKa values and tautomer populations in invisible protein states. P Natl Acad Sci Usa. **2014**, 111, 17, E1705-E1712. https://doi.org/10.1073/pnas.1400577111

[34]. Turi, I.; Kallay, C.; Szikszai, D.; Pappalardo, G.; Di Natale, G.; De Bona, P.; Rizzarelli, E.; Sovago, I. Nickel(II) complexes of the multihistidine peptide fragments of human prion protein. J Inorg Biochem. **2010**, 104,8, 885-891. https://doi.org/10.1016/j.jinorgbio.2010.04.008

[35]. Dolomanov, O.V., Bourhis, L.J., Gildea, R.J, Howard, J.A.K. & Puschmann, H. OLEX2: a complete structure solution, refinement and analysis program. J. Appl. Cryst. **2009**, 42, 339-341 https://doi.org/10.1107/S0021889808042726

[36]. Sheldrick, G.M. SHELXT - Integrated space-group and crystal-structure determination. Acta Cryst A71. **2015**, 3-8. https://doi.org/10.1107/S2053273314026370

[37]. Sheldrick, G.M. ShelXle: a Qt graphical user interface for SHELXL. Acta Cryst. A64. **2008**, 112-122. https://doi.org/10.1107/S0021889811043202

[38]. Chen, T.; Li, M.; Liu, J. π–π Stacking Interaction: A Nondestructive and Facile Means in Material Engineering for Bioapplications. Cryst Growth Des. **2018**, 18, 5, 2765-2783. https://doi.org/10.1021/acs.cgd.7b01503

[39]. Wheeler, S. E. Understanding Substituent Effects in Noncovalent Interactions Involving Aromatic Rings. Acc. Chem. Res. **2013**, 46, 4, 1029-1038. https://doi.org/10.1021/ar300109n

[40]. Iwunze, M. O. The characterization of the fluorescence of l-histidine in simulated body fluid. J Photoch Photobio A. **2007**, 18, 2-3, 283-289. https://doi.org/10.1016/j.jphotochem.2006.05.034

[41]. Wegeberg, C.; Wenger, O. S. Luminescent First-Row Transition Metal Complexes. J. Am. Chem. Soc. Au. **2021**, 1, 11, 1860-1876. https://doi.org/10.1021/jacsau.1c00353

[42]. Tao, B.; Cheng, F.; Jiang, X.; Xia, H. Synthesis, crystal structures and luminescent properties of nickel (II) and copper (II) hexaazamacrocyclic compounds with 1,3,5-benzenetricarboxylate ligands. J Mol Struct. **2012**, 1028, 176-180. https://doi.org/10.1016/j.molstruc.2012.06.043

[43]. Zhang, Z-H.; Li, X-Y.; Yang, X-S.; Chen, S-C.; Weng, Z.; He, M-Y. Distinct supramolecular assemblies of nickel(II) complexes constructed from N-(4-pyridylmethyl)-l-amino acid derivatives: Synergistic effects of substituent groups and counter anions. Polyhedron. **2018**, 148, 138-146. https://doi.org/10.1016/j.poly.2018.03.036

[44]. Rueff, J-M; Nierengarten, J –F.; Gilliot, P.; Demessence, A.; Cregut, O.; Drillon, M.; Rabu, P. Influence of Magnetic Ordering on the Luminescence in a Layered Organic−Inorganic OPV−Ni(II) Compound. Chem. Mater. **2004**, 16, 15, 2933-2937. https://doi.org/10.1021/cm049792c

[45]. Edvinsson, L.; Hakanson, R.; Ronnberg, A. L.; Sundler, F. Separation of histidyl-peptides by thin-layer chromatography and microspectrofluorometric characterization of their o-phthalaldehyde-induced fluorescence. J Chromatogr. **1972**, 67, 1, 81-5. https://doi.org/10.1016/S0021-9673(01)97150-X

[46]. Fukuda, M.; Hayashi, H.; Hasegawa, T.; Morii, T. Development of a fluorescent ribonucleopeptide sensor for histidine. T Mrs Jap. **2009**, 34, 3, 525-527. https://doi.org/10.14723/tmrsj.34.525

[47]. Goldman, E. R.; Medintz, I. L.; Hayhurst, A.; Anderson, G. P.; Mauro, J. M.; Iverson, B. L.; Georgiou, G.; Mattoussi, H. Self-assembled luminescent CdSe−ZnS quantum dot bioconjugates prepared using engineered poly-histidine terminated proteins. Anal Chim Acta. **2005**, 534, 1, 63-67. https://doi.org/10.1016/j.aca.2004.03.079

[48]. Song, L.; Xiao, J.; Cui, R.; Wang, X.; Tian, F.; Liu, Z. Eu3+ doped bismuth metal-organic frameworks with ultrahigh fluorescence quantum yield and act as ratiometric turn-on sensor for histidine detection. Sensor Actuat B-Chem. **2021**, 336, 129753-129761. https://doi.org/10.1016/j.snb.2021.129753

[49]. Zhang, S-T.; Li, P.; Liao, C.; Luo, T.; Kou, X.; Xiao, D. A highly sensitive luminescent probe based on Ru(II)-bipyridine complex for Cu2+, l-Histidine detection and cellular imaging. Spectrochim Acta A. **2018**, 201, 161-16. https://doi.org/10.1016/j.saa.2018.05.001

[50]. Nakamura, H.; Pisano, J. J. Fluorescamine derivatives of histidine, histamine and certain related imidazoles: Unique fluorescence after heating in acid. Arch Biochem Biophys. 1976, 177, 1, 334-5. https://doi.org/10.1016/0003-9861(76)90445-8

[51]. Li, J.; Ma, K-X.; Yang, Y.; Yang, H.; Lu, J.; Li, D-C.; Dou, J-M.; Ma, H-Y.; Wang, S-N.; Li, Y-W. A {Zn4} cluster as a bi-functional luminescence sensor for highly sensitive detection of chloride ions and histidine in aqueous media. J Mater Chem C. **2022**, 10, 23, 8979-8993. https://doi.org/10.1039/D2TC01610A

[52]. Yang, A-F.; Hou, S-L.; Shi, Y.; Yang, G-Li. Qin, D-B.; Zhao, B. Stable Lanthanide–Organic Framework as a Luminescent Probe to Detect Both Histidine and Aspartic Acid in Water. *Inorg. Chem.* **2019**, 58, 9, 6356-6362. https://doi.org/10.1021/acs.inorgchem.9b00562

[53]. Ledvina, M.; LaBella, F. S. Fluorescent substances in protein hydrolyzates I. Acid "Hydrolyzates" of individual amino acids Anal Biochem. **197**0, 36, 1, 174-81. https://doi.org/10.1016/0003-2697(70)90345-3

[54]. Loewenthal, R.; Sancho, J.; Fersht, A. R. Fluorescence spectrum of barnase: contributions of three tryptophan residues and a histidine-related pH dependence Biochemistry. **199**1, 30,27, 6775-9. https:// DOI:10.1021/bi00241a021

[55]. Jin, Y.; Gao, X. Plasmonic fluorescent quantum dots. Nat Nanotechnol. **2009**, 4, 9, 571-576. https://doi.org/10.1038/nnano.2009.193

[56]. Xiao, L.; Wei, P.; He, F.; Gou, Y.; Wang, P.; Yang, X. Rational design of dual-modalitye peptide-based probe for detection of Cu(II) and l-histidine in 100% aqueous solution and its application for living cells, test strips and smartphone. J Photoch Photobio A: Chemistry. **2023**, 442, 114762-114771. https://doi.org/10.1016/j.jphotochem.2023.114762

[57]. Yang, W.; Chen, X.; Su, H.; Fang, W.; Zhang, Y. The fluorescence regulation mechanism of the paramagnetic metal in a biological HNO sensor Chem Comm. **2015**, 51, 47, 9616-9619. https://doi.org/10.1039/C5CC00787A